Arabian Journal of Geosciences (2019) 12: 640
https://doi.org/10.1007/s12517-019-4769-2

ORIGINAL PAPER

# Relative influence of strength and geometric parameters on the behavior of jointed rock slopes

Nishant Roy[1] · Rajib Sarkar[2] · Shiv Dayal Bharti[1]

Received: 16 June 2016 / Accepted: 30 August 2019 / Published online: 17 October 2019


## Abstract

The assessment of performance of jointed rock slopes poses significant challenges due to the variable nature of geological material. A number of past investigations have incorporated the inherent variability in prediction of slope behavior through the use of probabilistic-based approaches. However, such investigations have primarily attempted to determine the probability of failure and rarely focused on the assessment of relative contribution of individual parameters on the slope behavior. In the present study, an efficient and robust way of determining the relative influence of variable strength and geometric parameters on slope behavior has been discussed. The effects of each individual parameter and their combined effect or interaction on slope stability have been highlighted. In addition, mathematical model (response surface) for prediction of slope behavior has been framed using the efficient central composite design (CCD) model. Moreover, adequacy of the present approach in identifying the influencing parameters has been highlighted. It is believed that the identification of influencing parameters using the present approach may help practitioners in choosing the appropriate measures for improving the stability of jointed rock slopes.

**Keywords** Rock slope · Impersistent joints · Central composite design · Response surface

## Introduction

The evaluation of stability of jointed rock slopes has been a complex and challenging task owing to the inherent variability associated with geological material. To effectively consider the risks arising from the associated uncertainties, probabilistic-based approach has been widely adopted in a number of investigations (Vanmarcke 1980, Oka and Wu 1990, Low and Einstein 1992, Christian et al. 1994, Low 1997, Juang et al. 1998, Duncan 2000, Park and West 2001, Duzgun et al. 2003, Park et al. 2005, Low 2007, Low 2008, Ching et al. 2009, Duzgun and Bhasin 2009, Li et al. 2011, Lee et al. 2012, Park et al. 2012). However, most of these probabilistic-based stability analyses of slopes have considered the variability only in terms of strength parameters, i.e., cohesion and friction angle of intact rock and the discontinuities or the rock mass, discarding other forms of uncertainties. Moreover, most of these investigations have concentrated mainly on the determination of probability of failure with very little focus on the relative contribution of various parameters on slope stability.

However, a prominent form of uncertainty in case of jointed rock slope arises from the scattered values of the geometric parameters (such as dip and trace length) of the discontinuities. In fact, the large number of case studies has highlighted dependency of stability of slopes on geometric parameters of geological structures (Fookes and Wilson 1966; Varnes 1978; Crozier 1986; Koukis and Ziourkas 1991; Guzzetti et al. 1996, Gunther 2003; Grelle et al. 2011, Maerz et al. 2015, Youssef et al. 2014, 2015). It is believed that the consideration of this form of geometric variability in stability assessment would be of practical significance. But this form of uncertainty has seldom been considered in the stability analysis barring a few cases (Hammah et al. 2009; Brideau et al. 2012; Shamekhi and Tannant 2015).

Responsible Editor: Zeynal Abiddin Erguler

✉ Rajib Sarkar
rajib@iitism.ac.in

Nishant Roy
nishantciv@gmail.com

Shiv Dayal Bharti
sdbharti@gmail.com

[1] Department of Civil Engg, MNIT Jaipur, Jaipur 302017, Rajasthan, India

[2] Department of Civil Engg, IIT(ISM) Dhanbad, Dhanbad 826004, Jharkhand, India

In the present study, the influence of uncertainty in strength parameters of the intact rock and the discontinuities along with the variability in geometric parameters of two impersistent joint sets on the stability of a rock slope has been investigated. The relative contribution of various parameters and their combined effect on the stability of a jointed rock slope has been evaluated and quantified through the use of the concepts of design of experiments (DOE) and ANOVA (Analysis of Variance) approaches. Moreover, a mathematical prediction model (response surface) for the expected strength reduction factor (SRF) over the range of parameters considered in the present study has been established. It is believed that the approach highlighted in the present study will help in gaining better insight into the behavior of rock slope. Such an approach will also help in identification of parameters which should be improved for better slope performance. Therefore, this approach will be beneficial for engineers in deciding measures to be adopted for improving the stability.

## Methodology

The methodology adopted in the present study is based on the application of the concepts of design of experiments (DOE) (Montgomery 2013) in a numerical framework. DOE provides a powerful tool to evaluate the cause-and-effect relation between the system response and the input parameters. For efficient implementation of the DOE approach, the factorial design has been adopted in the initial phase of the analysis using a finite element–based software package RS2.0 (Rocscience Inc., 2015). In this phase, also known as the factor screening phase, the parameters having significant influence on the behavior of considered slope, quantified in terms of SRF, are identified. In addition, the relative influence arising due to interaction among various parameters is also evaluated. Once the influencing parameters have been identified, the response surface describing the SRF of the slope are evaluated based on the central composite design model (Montgomery 2013). A step by step illustration of the adopted methodology is shown in Fig. 1. The results of the present study may be verified by following the steps provided in Fig. 1. A concise discussion of each component of the methodology is provided in subsequent sections.

## Concept of factorial design

Considering the objective of the present study, one of the main challenges requires efficient management of computational burden as large combination of input parameters are involved. For this purpose, the concept of factorial design has been considered for efficient implementation of numerical simulations.

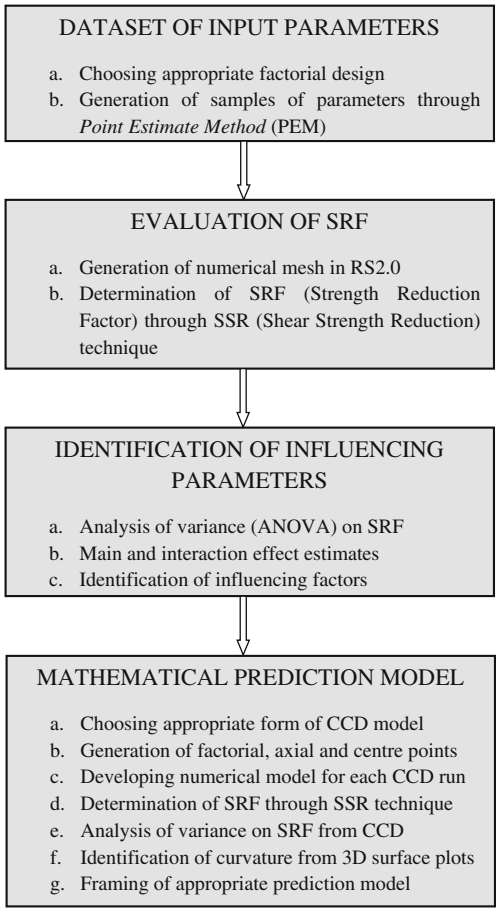


**Fig. 1** Flowchart depicting the steps adopted for the present study

Factorial design has been widely adopted to investigate the response of systems dependent on a large number of parameters. It provides a framework within which the joint effect of several parameters on system response is evaluated by carrying out the smallest number of experiments. Thus, it is widely used in screening of important factors while conducting experiments. Following the identification of influencing parameters, more rigorous analysis may be undertaken for developing the prediction model.

Among various cases of factorial designs, the $2^k$ designs, where $k$ denotes the number of random parameters, have found wide application in engineering studies. In such design, each parameter is assigned two levels: low and high. Thus, for a system dependent on $k$factors, $2^k$number of experiments is required to be conducted. However, in the case of a large number of parameters, half factorial design may be adopted which reduces the number of experiments to half of that required in case of full factorial design (Montgomery 2013).

In the initial factor screening phase, an assumption of linear variation in system response over the range of parameters is made. Although this assumption may not be exact, it is a reasonable simplification in the initial screening phase aimed towards the identification of the influencing parameters. Once

the effect of each parameter and their combined influences are known, more rigorous statistical analysis may be taken up to frame a relationship between the system response and the significant influencing parameters.

## Assessment of influence of various parameters

The effects of individual parameters and their combined influences on the response of a system may be summarized in the form of main and interaction effect estimates (Montgomery 2013). For clarity of the paper, a brief discussion dealing with the evaluation of these estimates is provided below.

Suppose the system response is dependent on three factors A, B, and C each at two levels: low and high denoted by − and + respectively. In such case, a $2^3$ factorial design may be adopted with a total of eight runs with parameter combinations as illustrated in Table 1. In any combination, the high level of a factor is defined by the corresponding lower case letter. By convention, (1) denotes the case where all the parameters are at their respective low levels. Thus, *ab* represents the case where factors A and B are at their corresponding high level and factor C is at low level. Similar convention may be extended for other labels. Figure 2 provides the various combinations possible in the case of $2^3$ factorial design with an illustration of the meaning of various labels.

The average effect of a factor on the response of a system is defined as the change in the response arising as a result of change in the level of that particular factor averaged over the levels of all other factors involved in the system. Thus, by definition, the average effect of A, also known as the main effect, may be evaluated using Eq. (1). The interpretation of each term of Eq. (1) is explained below.

$$A = \frac{1}{4n}[a-(1) + ab\text{-}b + ac\text{-}c + abc\text{-}bc] \tag{1}$$

The effect of A when both B and C are at low levels is given by $[a-(1)]/n$. In a similar way, the effect of A when B is at low level and C is at high level is given by $[ac-c]/n$. $[ab-b]/n$represents the effect of A when B is at high level and C is at low level. Finally, the effect of A when both B and C are at high levels is given by $[abc-bc]/n$. It should be noted that the term *n* denotes the number of replicates of the experiment. In case of no replication, the value of *n* becomes 1.

**Table 1** Combination of parameters in $2^3$ factorial design

| Run | A | B | C | Label |
|---|---|---|---|---|
| 1 | − | − | − | (1) |
| 2 | + | − | − | *a* |
| 3 | − | + | − | *b* |
| 4 | + | + | − | *ab* |
| 5 | − | − | + | *c* |
| 6 | + | − | + | *ac* |
| 7 | − | + | + | *bc* |
| 8 | + | + | + | *abc* |

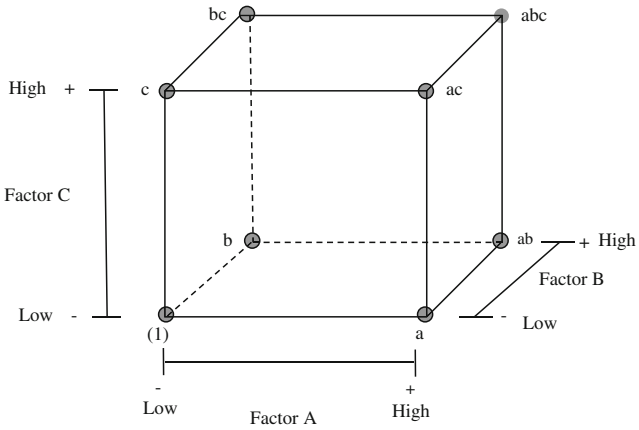


**Fig. 2** Various combinations of experiment run in a $2^3$ factorial design

In a similar way, the equations for main effects of factor B and C are given by Eqs. (2) and (3) respectively.

$$B = \frac{1}{4n}[b + ab + bc + abc-(1)-a-c-ac] \tag{2}$$

$$C = \frac{1}{4n}[c + ac + bc + abc-(1)-a-b-ab] \tag{3}$$

For interaction between two factors say AB, Eq. (4) is used. The interaction AB is the difference between the average effects of A at two levels of B. Similarly, Eqs. (5) and (6) are used for estimating the interaction effects of BC and AC respectively.

$$AB = \left[\frac{abc-bc- + ab-b-ac + c-a + (1)}{4n}\right] \tag{4}$$

$$BC = \frac{1}{4n}[(1) + a\text{-}b\text{-}ab\text{-}c\text{-}ac + bc + abc] \tag{5}$$

$$AC = [(1)-a + b\text{-}ab\text{-}c + ac\text{-}bc + abc] \tag{6}$$

For three-factor interaction ABC, Eq. (7) is applicable which denotes the average difference between the interaction term AB at two different levels of C.

$$ABC = \frac{[abc\text{-}bc\text{-}ac + c\text{-}ab + b + a-(1)]}{4n} \tag{7}$$

The terms in the brackets of Eqs. (1) to (7) are also known as the contrasts in the treatment combinations (Montgomery 2013). Using the contrasts, the sum of squares for the effect estimates may be evaluated as per Eq. (8). Based on the sum of squares of various terms, the percentage contribution towards the response may be evaluated.

$$SS = \frac{(Contrast)^2}{8n} \tag{8}$$

The concept discussed above for the case of three parameters may be extended for any number of parameters.

The present study has made use of the point estimate method (PEM) for the generation of samples required in the implementation of factorial design discussed above. A brief background of the original formulation of PEM along with the modification incorporated in the present study is discussed below.

## Generation of samples through point estimate method

As discussed in the previous section, the factorial design approach requires the determination of response at various combinations of factors. One of the efficient ways of achieving this is with the application of point estimate method developed by Rosenblueth (1975). As per the original formulation, each random parameter is represented by two point estimates (Baecher and Christian 2003): low and high, given by Eq. (9)

$$\chi^{+} = \mu_{\chi} + \sigma_{\chi} \tag{9}$$

where $\mu_x$ is the mean and $\sigma_x$ is the standard deviation of parameter $X$. For a more detailed discussion on the application of the point estimate method in the probabilistic analysis of rock slopes, the work of Ahmadabadi and Poisel (2016) may be referred. The above study highlights and summarizes advantages, limitations, and modifications to be made to the original formulation depending on the characteristic of the data considered. In the present study, the original formulation represented by Eq. (9) has been used for strength parameters. However, for geometric parameters, a modification incorporating the proposed improvement suggested by Hong (1996, 1998) is considered for the determination of point estimates as more than one skewed variables are involved. Thus, the point estimates in the present study are evaluated using Eq. (10) for skewed variables.

$$x_i^{+} = \mu_{xi} + \left[ v_{xi}/2 + \sqrt{n_s + (v_{xi}/2)^2} \right] \sigma_{xi} \tag{10}$$

where $\mu_{xi}$, $v_{xi}$, and $\sigma_{xi}$ represent the mean, skewness, and standard deviation of parameter $x_i$. The term $n_s$ in the above equation represents the number of skewed parameters considered in the analysis.

## Evaluation of strength reduction factor (SRF) of slope

The stability of the slope has been evaluated by determining the strength reduction factor (SRF) (Zienkiewicz et al. 1975, Naylor 1982, Donald and Giam 1988, Matsui and San 1992, Ugai and Leshchinsky 1995, Dawson et al. 1999, Griffiths and Lane 1999, Cheng et al. 2007, Wei et al. 2009, Fahimifar et al. 2012, Alemdag et al., 2014, Cai and Ugai 2000, Won et al. 2005, Wei and Cheng 2009, Griffiths et al. 2010, Yang et al. 2011, Rathod and Rao 2012, Shooshpasha and Amirdehi 2015, Zhang et al. 2015). For this, two-dimensional numerical modeling has been carried out using the finite element software RS2.0 (Rocscience Inc. 2015). This software package has been widely used in a number of numerical studies dealing with rock slope stability assessment through the Shear Strength Reduction (SSR) technique. Both persistent and impersistent joint sets along with widely adopted constitutive models for simulating rock mass behavior may be considered in this software package.

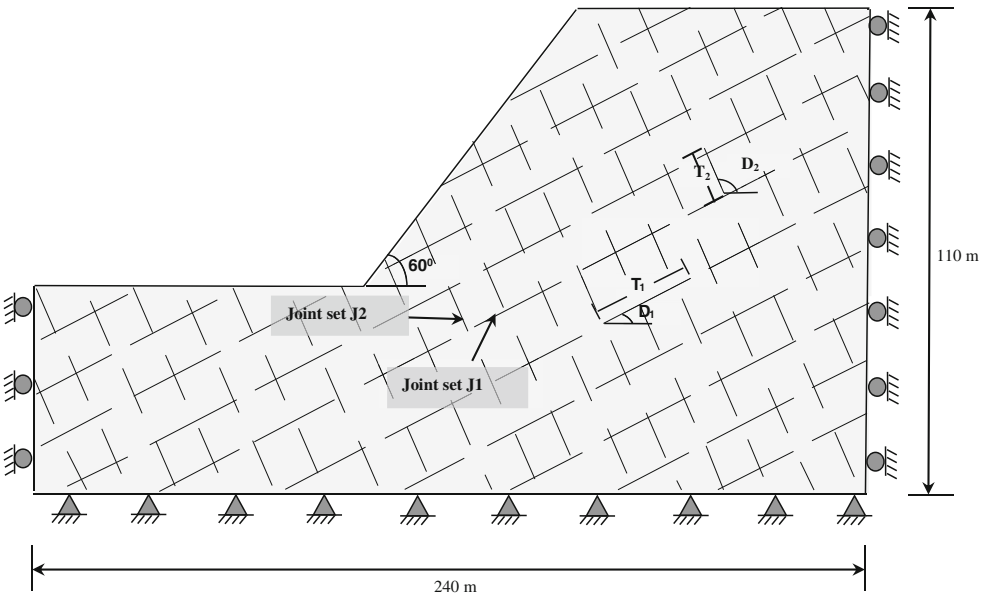


**Fig. 3** A schematic representation of the slope considered

**Table 2** Deterministic parameters considered (adapted after Hammah et al. 2009)

| Parameter | Intact rock |
|---|---|
| Unit weight of intact rock (kN/m$^3$) | 27.4 |
| Elastic modulus, $E$ (GPa) | 20.0 |
| Poisson's ratio, $\nu$ | 0.25 |
| Spacing, joint set J1 (m) | 2.0 |
| Spacing, joint set J2 (m) | 1.5 |
| In situ stress ratio, $K$ | 1.0 |
| Tensile strength, peak (MPa) | 0.3 |
| Tensile strength, residual (MPa) | 0.0 |

## Numerical model

A schematic representation of the slope having two impersistent joint sets considered in the present study is shown in Fig. 3. The slope geometry has been adapted from the study carried out by Hammah et al. (2009). The slope has a height of 60 m and a slope angle of 60° with two impersistent joint sets J1 and J2. The spacing of the first joint set J1 is 2 m and that of the second joint set J2 is 1.5 m. In order to minimize the effect of artificial boundaries, the model dimensions have been kept as 240 m × 110 m (Wyllie and Mah 2004). The bottom boundary of the model has been fixed in all directions, whereas the lateral boundaries have been restrained in the horizontal directions. Mohr-Coulomb constitutive law has been considered for both the intact rock and the impersistent joint sets. In all the analyses, the horizontal to vertical stress ratio has been fixed as 1.0. The number of elements used in each model has been decided based on mesh sensitivity analyses. Values of various deterministic parameters are summarized in Table 2.

## Random parameters considered in the study

In the present study, the variability in terms of spatial configuration of two impersistent joint sets J1 and J2 has been characterized in terms of dip angle $D_1$ and $D_2$, the trace length $T_1$ and $T_2$ respectively as shown in Fig. 3. Moreover, the stochastic nature of the strength parameters is represented by cohesion $C_i$ and friction angle $\phi_i$ for the intact rock and friction angle $\phi_j$ for the two joint sets. Thus, there are seven random parameters which have been considered for the initial factor screening phase and have been mentioned below for brevity.

1. Dip angle $D_1$ of the first joint set
2. Trace length $T_1$ of the first joint set
3. Dip angle $D_2$ of the second joint set
4. Trace length $T_2$ of the second joint set
5. Cohesion of intact rock $C_i$
6. Friction angle of intact rock $\phi_i$
7. Friction angle of the first and second joint set $\phi_j$

Consideration of seven random parameters in full factorial design requires simulation of total 128 ($2^7$) numerical models. Since the number of simulation is quite large, half factorial design has been considered as has been done in many cases of design of experiments. This brings down the total number simulations to 64 in the initial factor screening phase.

## Distribution type and properties for random parameters

The choice of type of statistical distribution for random parameters has been made based on the suggestions made in a number of studies. Normal and truncated normal distribution has been suggested for the friction angle of the rock discontinuities and the intact rock (Mostyn and Li 1993, Nilsen 2000, Pathak and Nilsen 2004). Cohesion for rock is also reported to follow a normal distribution (Song et al. 2011). As per Priest (1993), Fisher distribution is capable to model the dip of discontinuities with considerable accuracy. In addition, the trace length is assumed to follow lognormal distribution (Bridges 1976, Priest and Hudson 1976, Baecher et al., 1977, Baecher and Lanney, 1978, Warburton 1980, Hudson and Priest 1983, Baecher, 1983, Dershowitz and Einstein 1988, Ehlen 2002, Meyer and Einstein 2002, Gumede and Stacey 2007, Weiss 2008, Zadhesh et al. 2014). In view of the aforementioned studies, the distribution of each random parameter along with the properties considered in the investigation is presented in Table 3.

**Table 3** Random parameters adopted in the present study

| Random parameters | Distribution | Skewness | Mean (μ) | Standard deviation (σ) | Point Estimate (−) | Point Estimate (+) |
|---|---|---|---|---|---|---|
| $D_1$(in deg) | Weibull | − 1 | 40 | 8 | 19.5 | 52.5 |
| $T_1$(m) | Lognormal | 0.6 | 10 | 1.5 | 7.5 | 13.5 |
| $D_2$(in deg) | Weibull | − 0.6 | 110 | 4 | 101 | 117 |
| $T_2$ (m) | Lognormal | 0.3 | 6 | 0.5 | 5 | 7 |
| $C_i$(MPa) | Normal | – | 1 | 0.3 | 0.7 | 1.3 |
| $\phi_i$(in deg) | Normal | – | 30 | 6 | 24 | 36 |
| $\phi_j$(in deg) | Normal | – | 20 | 4 | 16 | 24 |

**Table 4** Model runs and corresponding SRF for the initial factor screening phase

| Model run | $D_1$ | $T_1$ | $D_2$ | $T_2$ | $C_i$ | $\Phi_i$ | $\Phi_j$ | SRF |
|---|---|---|---|---|---|---|---|---|
| 1 | − | − | − | − | − | − | + | 1.54 |
| 2 | + | − | − | − | − | − | − | 1.00 |
| 3 | − | + | − | − | − | − | − | 0.89 |
| 4 | + | + | − | − | − | − | + | 0.89 |
| 5 | − | − | + | − | − | − | − | 1.02 |
| 6 | + | − | + | − | − | − | + | 1.14 |
| 7 | − | + | + | − | − | − | + | 1.16 |
| 8 | + | + | + | − | − | − | − | 0.75 |
| 9 | − | − | − | + | − | − | − | 1.10 |
| 10 | + | − | − | + | − | − | + | 1.10 |
| 11 | − | + | − | + | − | − | + | 1.40 |
| 12 | + | + | − | + | − | − | − | 0.58 |
| 13 | − | − | + | + | − | − | + | 0.93 |
| 14 | + | − | + | + | − | − | − | 0.76 |
| 15 | − | + | + | + | − | − | − | 0.70 |
| 16 | + | + | + | + | − | − | + | 0.83 |
| 17 | − | − | − | − | + | − | − | 1.12 |
| 18 | + | − | − | − | + | − | + | 1.24 |
| 19 | − | + | − | − | + | − | + | 1.36 |
| 20 | + | + | − | − | + | − | − | 0.72 |
| 21 | − | − | + | − | + | − | + | 1.37 |
| 22 | + | − | + | − | + | − | − | 1.00 |
| 23 | − | + | + | − | + | − | − | 0.91 |
| 24 | + | + | + | − | + | − | + | 0.95 |
| 25 | − | − | − | + | + | − | + | 1.56 |
| 26 | + | − | − | + | + | − | − | 0.86 |
| 27 | − | + | − | + | + | − | − | 0.97 |
| 28 | + | + | − | + | + | − | + | 0.78 |
| 29 | − | − | + | + | + | − | − | 0.71 |
| 30 | + | − | + | + | + | − | + | 1.10 |
| 31 | − | + | + | + | + | − | + | 0.98 |
| 32 | + | + | + | + | + | − | − | 0.64 |
| 33 | − | − | − | − | − | + | − | 1.11 |
| 34 | + | − | − | − | − | + | + | 1.23 |
| 35 | − | + | − | − | − | + | + | 1.37 |
| 36 | + | + | − | − | − | + | − | 0.71 |
| 37 | − | − | + | − | − | + | + | 1.38 |
| 38 | + | − | + | − | − | + | − | 0.96 |
| 39 | − | + | + | − | − | + | − | 0.91 |
| 40 | + | + | + | − | − | + | + | 0.95 |
| 41 | − | − | − | + | − | + | + | 1.54 |
| 42 | + | − | − | + | − | + | − | 0.87 |
| 43 | − | + | − | + | − | + | − | 0.97 |
| 44 | + | + | − | + | − | + | + | 0.78 |
| 45 | − | − | + | + | − | + | − | 0.70 |
| 46 | + | − | + | + | − | + | + | 1.00 |
| 47 | − | + | + | + | − | + | + | 0.94 |
| 48 | + | + | + | + | − | + | − | 0.64 |
| 49 | − | − | − | − | + | + | + | 1.57 |
| 50 | + | − | − | − | + | + | − | 0.99 |
| 51 | − | + | − | − | + | + | − | 0.92 |
| 52 | + | + | − | − | + | + | + | 0.93 |
| 53 | − | − | + | − | + | + | − | 1.01 |
| 54 | + | − | + | − | + | + | + | 1.31 |
| 55 | − | + | + | − | + | + | + | 1.26 |
| 56 | + | + | + | − | + | + | − | 0.82 |
| 57 | − | − | − | + | + | + | − | 1.10 |
| 58 | + | − | − | + | + | + | + | 1.11 |
| 59 | − | + | − | + | + | + | + | 1.42 |
| 60 | + | + | − | + | + | + | − | 0.58 |
| 61 | − | − | + | + | + | + | + | 0.94 |
| 62 | + | − | + | + | + | + | − | 0.79 |
| 63 | − | + | + | + | + | + | − | 0.70 |
| 64 | + | + | + | + | + | + | + | 0.89 |

## SRF from numerical model

The results of the initial factor screening phase implemented with the help of numerical models based on half factorial design are discussed in terms of SRF (strength reduction factor) in the present section. Table 4 summarizes the 64 runs made with various combinations of input random parameters. The corresponding factor of safety of the slope for each run has been shown as SRF in the last column. It may be noted that the minimum SRF of the slope is 0.58 (model run 12), whereas the maximum SRF is 1.57 (model run 49).

In the case of the lowest SRF (model run 12), the strength parameters of the intact rock and the discontinuity are minimum, whereas the dip angle and the trace length of joint set 1 have maximum value. In comparison, the case of highest SRF (model run 49) is associated with maximum point estimate for the strength parameters and minimum point estimates for the geometric parameters of joint set J1. In order to quantify the effect of each individual parameter and the combined effect or interaction among them on SRF of the slope, ANOVA (analysis of variance) has been carried out.

## Assessment of effects of random parameters

Based on the results of the initial 64 numerical simulations, the main and interaction effects have been identified through the analyses of SRF utilizing the concepts discussed in the "Concept of factorial design" section. Figure 4 shows the effect of each parameter on the SRF of the considered slope.

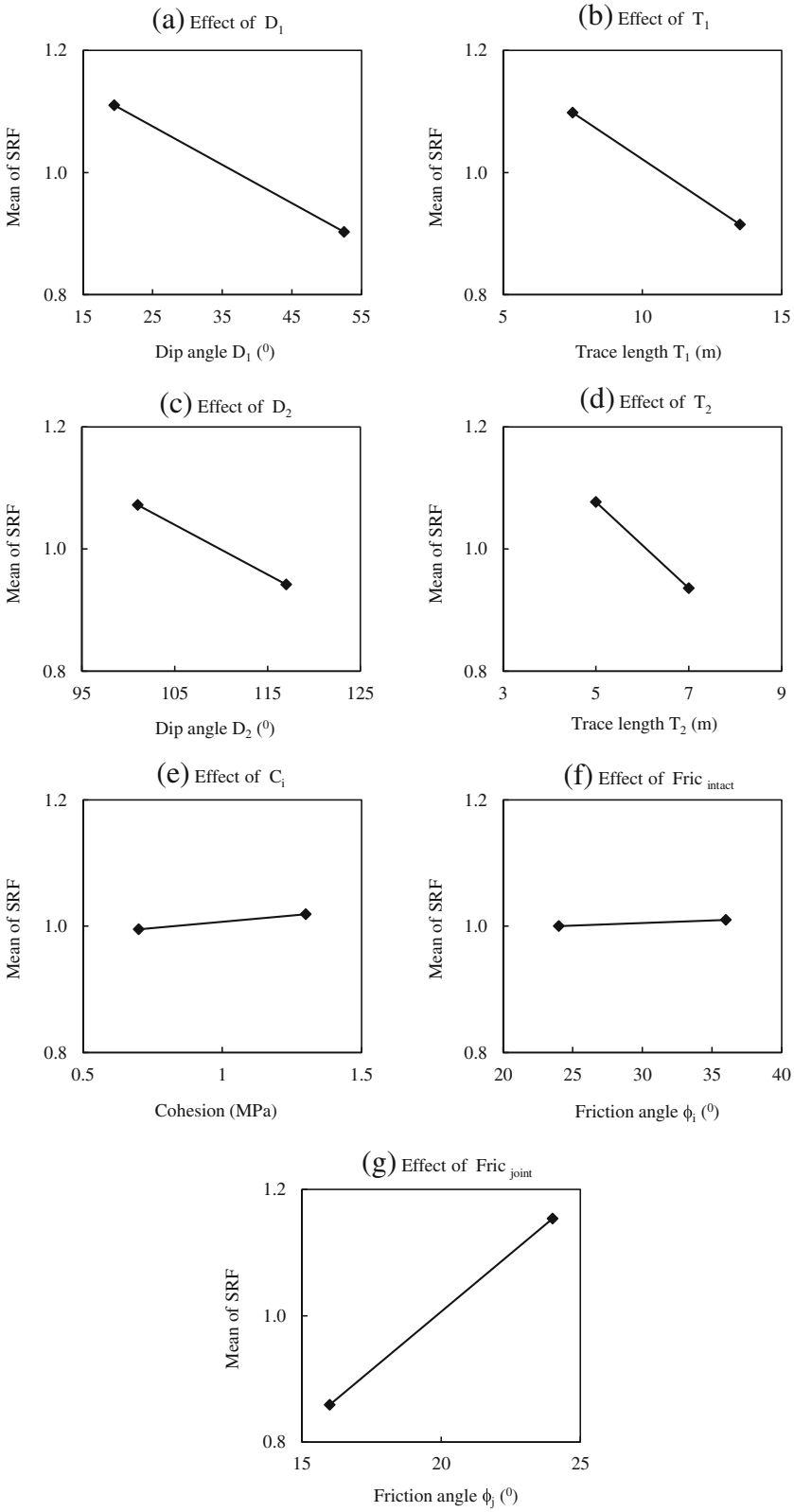


**Fig. 4** Effect of various random parameters on the SRF of the jointed rock slope. Effect of $D_1$ (**a**), effect of $T_1$ (**b**), effect of $D_2$ (**c**), effect of $T_2$ (**d**), effect of $C_i$ (**e**), effect of $Fric_{intact}$ (**f**), effect of $Fric_{joint}$ (**g**)

From Fig. 4a to d, it may be observed that the dip and trace length of both the first and second joint set are having significant influence on the SRF of the slope as with variation these parameters may make the slope unstable (SRF < 1). In addition, the friction angle of the joint sets also has significant impact on the stability as evident from Fig. 4g.

In contrast, Fig. 4e and f suggest that change in SRF is very minor within the range of the strength parameters of intact rock

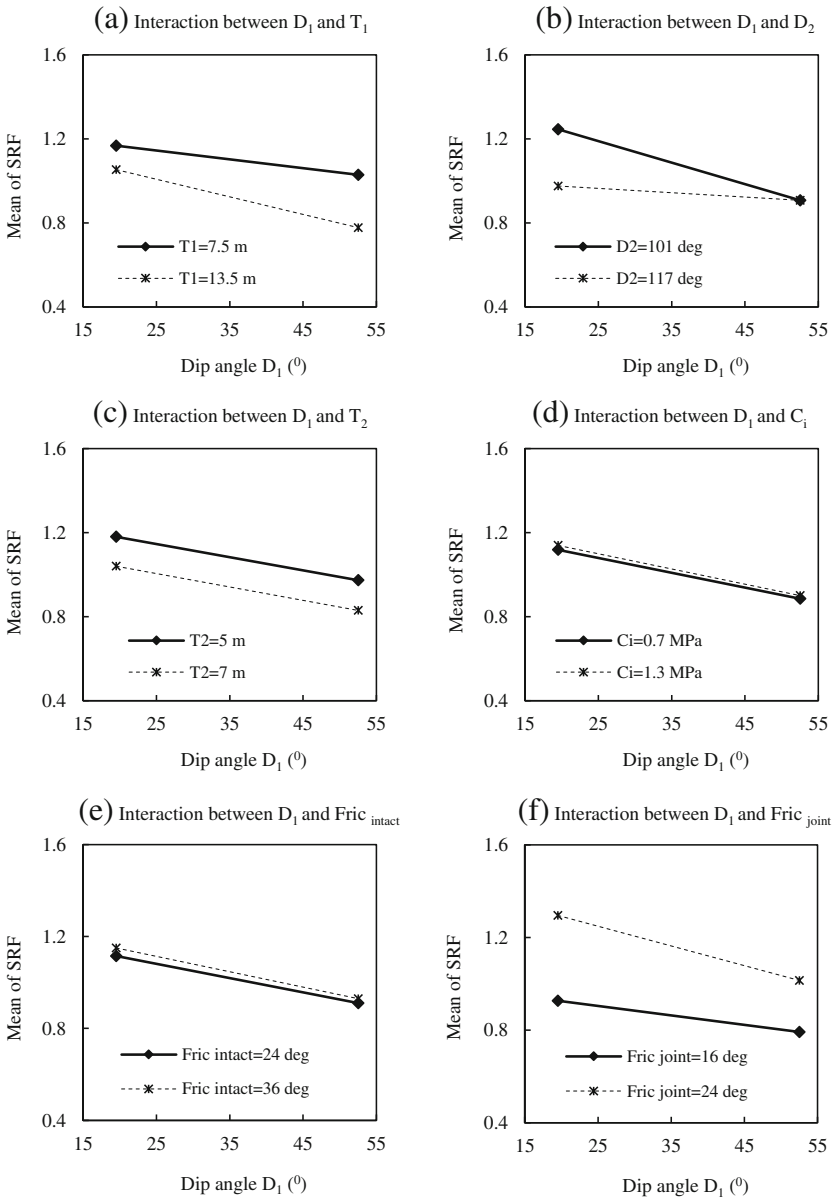


**Fig. 5** Combined effect of dip angle of the first joint set ($D_1$) with other random parameters. Interaction between $D_1$ and $T_1$ (**a**), interaction between $D_1$ and $D_2$ (**b**), interaction between $D_1$ and $T_2$ (**c**), interaction between $D_1$ and $C_i$ (**d**), interaction between $D_1$ and $Fric_{intact}$ (**e**), interaction between $D_1$ and $Fric_{joint}$ (**f**)

considered for the study. Thus, it may be concluded that cohesion $C_i$ and friction angle $\phi_i$ of intact rock do not have significant influence on the SRF. This finding may also be substantiated by comparing the results of model run 1 and model run 49 (refer to Table 4) where the intact rock strength properties are different, while the geometric and strength properties of the joint sets are same. A minor variation of 0.03 (1.57–1.54) in SRF is observed.

## Assessment of combined effects of random parameters

Figure 5 presents the combined effect of the first joint set dip angle with other random parameters on the mean of the SRF of the slope. It may be understood that the interaction effect will be prominent if the plots are having higher difference in gradients. Figure 5 indicates that there is a significant influence of combined effect of the following parameters with the dip angle of the first joint set ($D_1$): trace length of the first joint set ($D_1T_1$), dip angle of the second joint set ($D_1D_2$), joint friction angle ($D_1\phi_j$). All other interaction plots have slopes which are almost parallel thereby indicating that they do not influence the SRF.

Similarly, Fig. 6 represents the combined effect of the trace length of the first joint set ($T_1$) with other random parameters. Most of the plots shown are parallel indicating very minor combined influence of various random parameters with trace length $T_1$. However, Fig. 6a shows relatively higher difference in gradient indicating that there may be contribution of combined effect of dip angle of the first joint set with $T_1$ ($D_1T_1$).

Similarly, combined effect of other parameters has been shown in Figs. 7, 8, 9, and 10. The gradient of the interaction

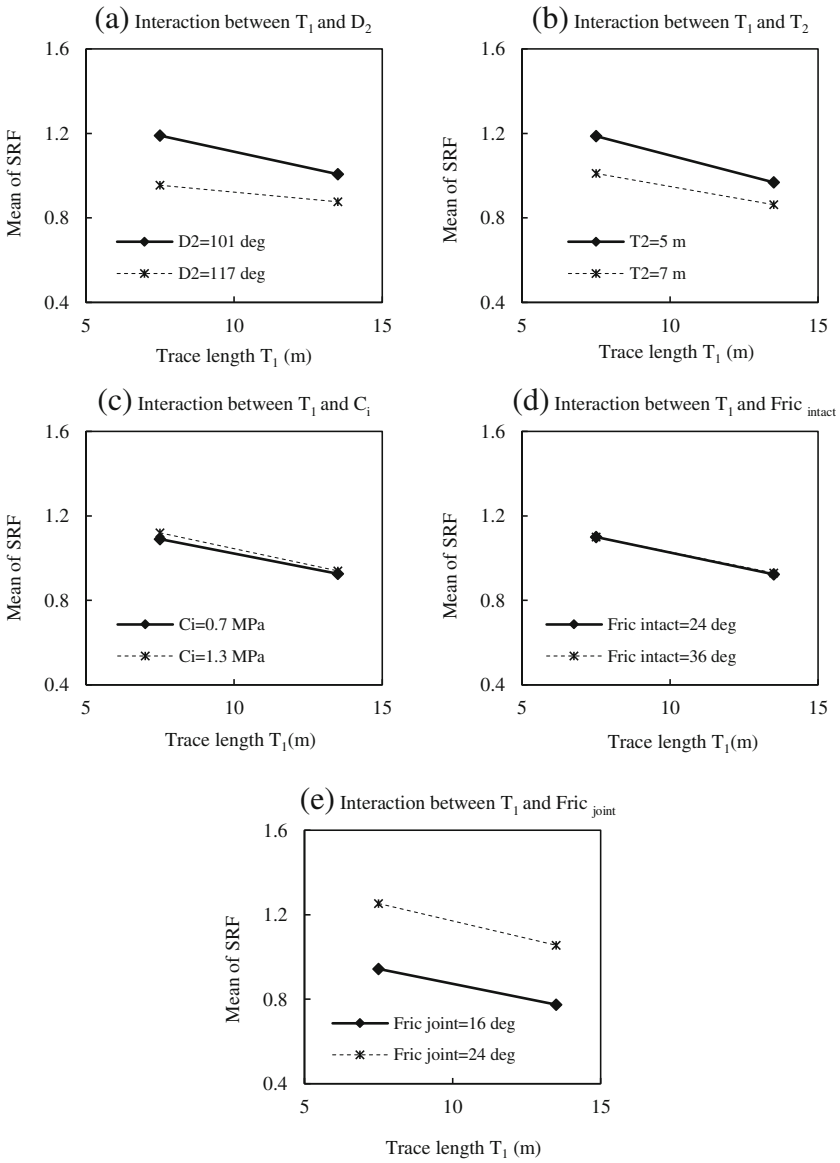


**Fig. 6** Combined effect of trace length of the first joint set ($T_1$) with other random parameters. Interaction between $T_1$ and $D_2$ (**a**), interaction between $T_1$ and $T_2$ (**b**), interaction between $T_1$ and $C_i$ (**c**), interaction between $T_1$ and $Fric_{intact}$ (**d**), interaction between $T_1$ and $Fric_{joint}$ (**e**)

plot (Fig. 7a) signifies that the SRF of the slope is dependent on the combined effect of dip angle and trace length of the second joint set ($D_2T_2$). Moreover, Fig. 7d also suggests that there may be combined effect of dip angle of the second joint set with joint friction angle ($D_2\phi_j$). Apart from the above-mentioned plots, all other interaction plots being parallel signify negligible combined effect.

## Quantitative assessment of effects of random parameters

The main and combined effects of various random parameters, presented in Figs. 4, 5, 6, 7, 8, 9, and 10, may further be quantified as discussed in the "Assessment of influence of various parameters" section. Table 5 summarizes the results of ANOVA in terms of the effect estimate, percentage contribution, $p$ value, and $F_o$ for all the main and interaction terms considered in the present work.

It may be observed that joint friction angle has maximum influence on the SRF of the slope. The percentage contribution for joint friction angle is estimated to be 35.49%. Next, higher contribution comes from dip angle and trace length of joint set J1 which characterize geometric properties. In addition, dip angle and trace length of joint set J2 also seem to have significant contribution in influencing stability of slope. Among the interaction terms, the combined effect of dip angle of both the joint sets ($D_1D_2$) has the maximum influence.

Further, the significance of each parameter is evaluated through the Fisher statistic $F_0$ keeping the significance level as 0.05 (Montgomery 2013). Based on the $F_0$ value, the significant parameters identified are $D_1$, $T_1$, $D_2$, $T_2$, and $\phi_j$.

However, the quantification presented in this section requires a closer scrutiny as these results are based on

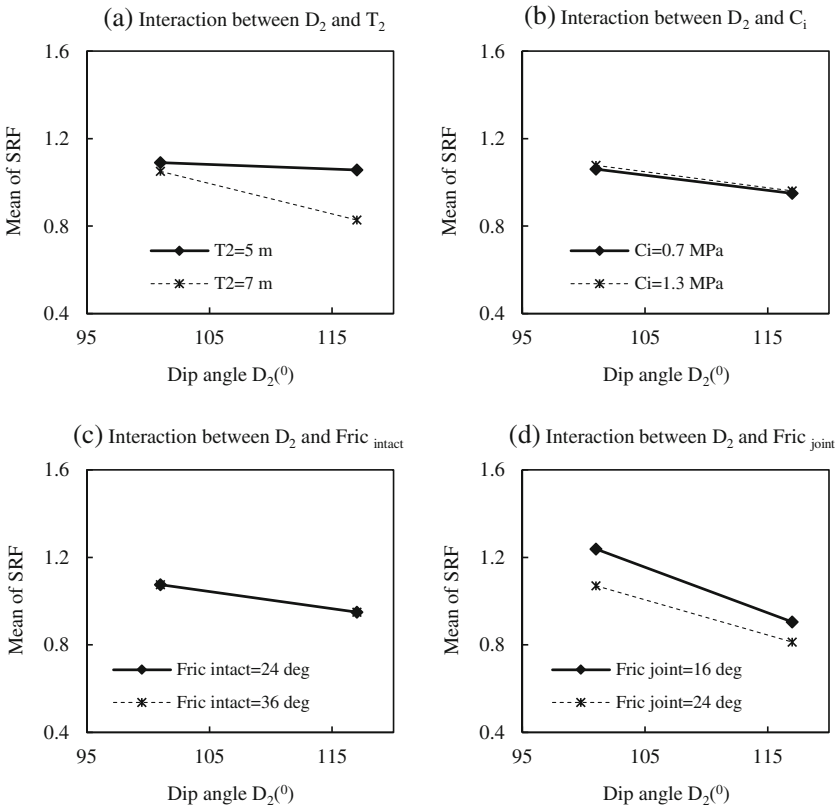


**Fig. 7** Combined effect of dip angle of the second joint set ($D_2$) with other random parameters. Interaction between $D_2$ and $T_2$ (**a**), interaction between $D_2$ and $C_i$ (**b**), interaction between $D_2$ and $Fric_{intact}$ (**c**), interaction between $D_2$ and $Fric_{joint}$ (**d**)

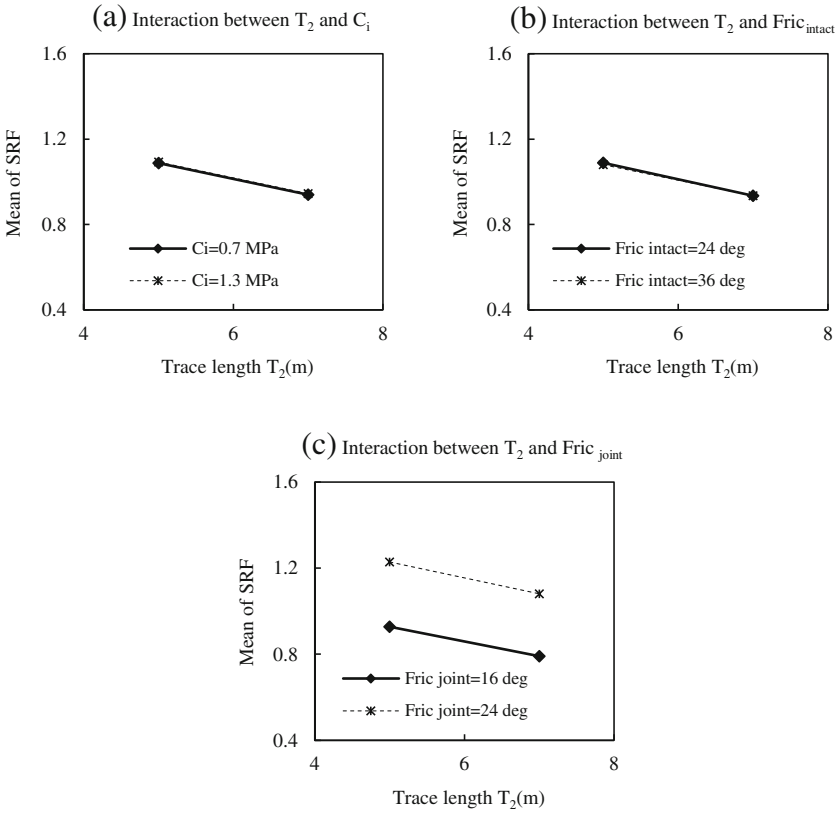


**Fig. 8** Combined effect of trace length of the second joint set ($T_2$) with other random parameters. Interaction between $T_2$ and $C_i$ (**a**), interaction between $T_2$ and $Fric_{intact}$ (**b**), interaction between $T_2$ and $Fric_{joint}$ (**c**)

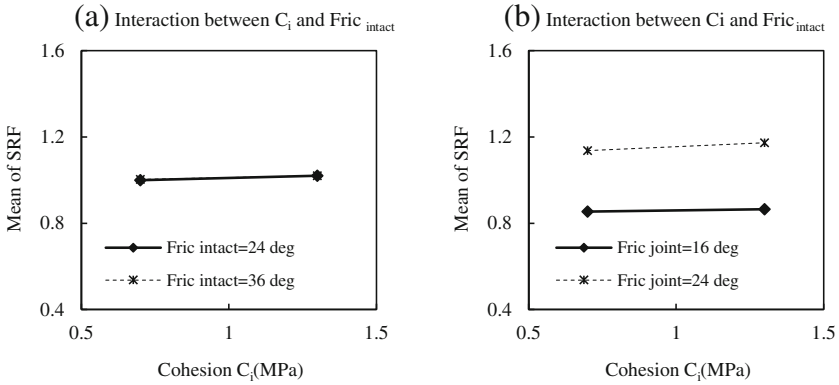


**Fig. 9** Combined effect of cohesion of intact rock ($C_i$) with random parameters. Interaction between $C_i$ and $Fric_{intact}$ (**a**), interaction between $C_i$ and $Fric_{intact}$ (**b**)

the assumption of linear variation of SRF. Hence, more accurate quantitative assessment may be made by identifying curvature effects, if any, based on the influencing parameters identified at this stage. For this purpose, central composite design (CCD) is implemented subsequently by taking into consideration the important influencing parameters identified at this stage. Further, a mathematical model (response surface) capable of predicting the SRF of the considered slope has been framed.

## Response surface using central composite design

The initial factor screening phase discussed in the "Assessment of effects of random parameters" section identifies the parameters affecting the stability of slope with an assumption of linear variation of SRF within the range of random parameters considered. However, the assumption of linear variation may not be accurate, and hence, a more rigorous analysis needs to be conducted to identify and account for the curvature effect, if any, on the SRF. In this regard, the central composite design (CCD), which is one of the most versatile models for evaluating the second order response

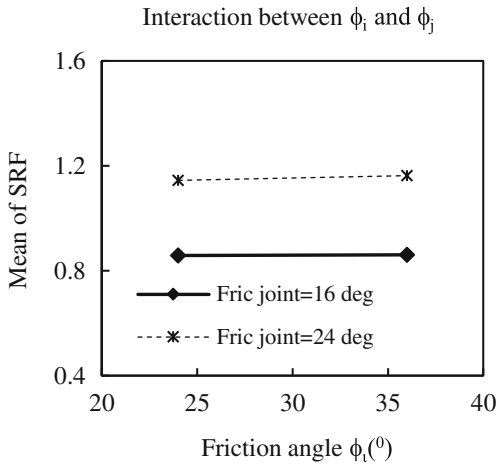


**Fig. 10** Combined effect of friction angle of intact rock ($\phi_i$) with joint friction angle ($\phi_j$)

**Table 5** ANOVA analysis on the SRF values from the initial factor screening phase

| Factor | Effect estimate | Sum of squares | Percentage contribution (%) | $p$ value | $F_o$ |
|---|---|---|---|---|---|
| $D_1$ | − 0.21 | 1.38 | 17.65 | 0.00 | 157.10 |
| $T_1$ | − 0.18 | 1.08 | 13.7 | 0.00 | 122.02 |
| $D_2$ | − 0.13 | 0.54 | 6.92 | 0.00 | 61.53 |
| $T_2$ | − 0.14 | 0.64 | 8.16 | 0.00 | 72.63 |
| $C_i$ | 0.02 | 0.02 | 0.23 | 0.16 | 2.08 |
| $\phi_i$ | 0.01 | 0.00 | 0.05 | 0.52 | 0.42 |
| $\phi_j$ | 0.30 | 2.78 | 35.49 | 0.00 | 315.76 |
| $D_1T_1$ | − 0.07 | 0.15 | 1.90 | 0.00 | 16.93 |
| $D_1D_2$ | 0.14 | 0.63 | 7.98 | 0.00 | 71.03 |
| $D_1T_2$ | 0.00 | 0.00 | 0.00 | 0.93 | 0.01 |
| $D_1C_i$ | 0.01 | 0.00 | 0.03 | 0.60 | 0.29 |
| $D_1\phi_i$ | 0.00 | 0.00 | 0.00 | 0.84 | 0.04 |
| $D_1\phi_j$ | − 0.07 | 0.17 | 2.15 | 0.00 | 19.17 |
| $T_1D_2$ | 0.05 | 0.09 | 1.13 | 0.00 | 10.07 |
| $T_1T_2$ | 0.04 | 0.04 | 0.51 | 0.04 | 4.49 |
| $T_1C_i$ | 0.00 | 0.00 | 0.00 | 0.93 | 0.01 |
| $T_1\phi_i$ | 0.01 | 0.00 | 0.02 | 0.69 | 0.16 |
| $T_1\phi_j$ | − 0.02 | 0.01 | 0.09 | 0.38 | 0.8 |
| $D_2T_2$ | − 0.09 | 0.24 | 3.07 | 0.00 | 27.32 |
| $D_2C_i$ | 0.01 | 0.01 | 0.08 | 0.40 | 0.73 |
| $D_2\phi_i$ | 0.01 | 0.00 | 0.01 | 0.77 | 0.09 |
| $D_2\phi_j$ | − 0.04 | 0.05 | 0.59 | 0.03 | 5.24 |
| $T_2C_i$ | − 0.01 | 0.00 | 0.01 | 0.73 | 0.12 |
| $T_2\phi_i$ | − 0.01 | 0.01 | 0.07 | 0.45 | 0.58 |
| $T_2\phi$j | − 0.01 | 0.00 | 0.01 | 0.74 | 0.11 |
| $C_i\phi_i$ | − 0.01 | 0.00 | 0.02 | 0.72 | 0.13 |
| $C_i\phi_j$ | 0.01 | 0.01 | 0.07 | 0.44 | 0.61 |
| $\phi_i\phi_j$ | 0.01 | 0.00 | 0.02 | 0.66 | 0.20 |

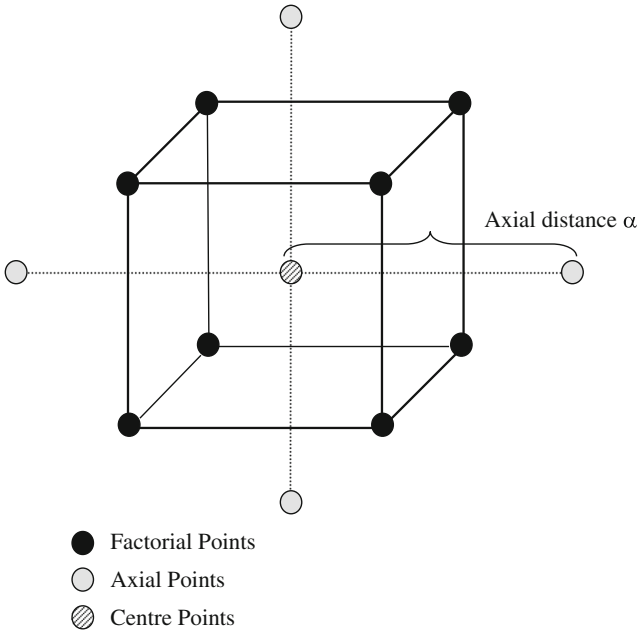


**Fig. 11** Design points in CCD model for the case of three parameters

surface, has been used (Box and Wilson 1951, Myers et al. 2004, Myers et al. 2009).

## Background of CCD

The popularity of CCD is primarily attributed to its sequential nature which enables the partitioning of the design into two subsets. The first subset is utilized to estimate the linear and two-factor interaction estimates. If the results from the analysis of the first subset indicate the presence of significant curvature in the response, the second subset is then run to estimate the curvature effects.

A schematic representation of CCD for three parameters has been shown in Fig. 11. In the case of $k$ factors, the design involves $2^k$ factorial points, $2k$ axial point, and $n'$ ($n'$ is variable) center points with the first order variation in the model represented by the factorial points. In case of existence of significant curvature, the axial points are used for the efficient determination of the quadratic terms. The axial point is dependent on a parameter $\alpha$ which denotes the axial distance from the center point. Thus, the CCD facilitates in identification of nature of variation of the response as a function of various input parameters.

## Application of CCD in the present study

In the present study, since five parameters are identified to be significant, the CCD model comprises $2^5$ (32) factorial points, $2 \times 5$ (10) axial points, and center points (equal to mean value). The axial distance $\alpha$ is evaluated using the relation $\alpha = \sqrt[4]{2^N}$, where $N$ represents the number of significant

**Table 6** SRF for the central composite design (CCD)

| Analyses | $D_1$ | $T_1$ | $D_2$ | $T_2$ | $\phi_j$ | SRF |
|---|---|---|---|---|---|---|
| CCD1 | − | − | − | − | − | 1.13 |
| CCD2 | 0 | 0 | 0 | −α | 0 | 0.68 |
| CCD3 | − | + | − | + | − | 0.97 |
| CCD4 | + | + | − | − | + | 0.92 |
| CCD5 | + | − | − | − | − | 1.13 |
| CCD6 | − | + | + | − | + | 1.25 |
| CCD7 | − | − | − | + | + | 1.49 |
| CCD8 | + | − | + | + | − | 0.72 |
| CCD9 | + | + | + | − | − | 0.8 |
| CCD10 | − | − | − | + | − | 1.13 |
| CCD11 | 0 | 0 | −α | 0 | 0 | 0.75 |
| CCD12 | 0 | α | 0 | 0 | 0 | 0.61 |
| CCD13 | − | − | + | − | − | 1.03 |
| CCD14 | − | − | − | − | + | 1.6 |
| CCD15 | 0 | 0 | 0 | 0 | 0 | 0.79 |
| CCD16 | + | + | − | − | − | 0.71 |
| CCD17 | 0 | 0 | 0 | 0 | 0 | 0.79 |
| CCD18 | 0 | 0 | 0 | 0 | 0 | 0.79 |
| CCD19 | 0 | 0 | 0 | 0 | +α | 0.54 |
| CCD20 | 0 | 0 | 0 | 0 | 0 | 0.79 |
| CCD21 | 0 | 0 | 0 | 0 | 0 | 0.79 |
| CCD22 | + | + | + | − | + | 1.00 |
| CCD23 | 0 | −α | 0 | 0 | 0 | 1.16 |
| CCD24 | 0 | 0 | 0 | 0 | 0 | 0.79 |
| CCD25 | − | − | + | + | + | 1.00 |
| CCD26 | −α | 0 | 0 | 0 | 0 | 2.2 |
| CCD27 | − | + | − | + | + | 1.49 |
| CCD28 | + | − | − | − | + | 1.24 |
| CCD29 | + | − | + | + | + | 0.94 |
| CCD30 | 0 | 0 | 0 | 0 | 0 | 0.79 |
| CCD31 | − 1 | 1 | 1 | 1 | − 1 | 0.71 |
| CCD32 | + | − | + | − | + | 1.17 |
| CCD33 | 0 | 0 | α | 0 | 0 | 0.75 |
| CCD34 | + | + | − | + | + | 0.80 |
| CCD35 | − | + | + | + | + | 1.00 |
| CCD36 | − | − | + | + | − | 0.71 |
| CCD37 | 0 | 0 | 0 | 0 | 0 | 0.79 |
| CCD38 | + | − | + | − | − | 0.92 |
| CCD39 | − | + | − | − | + | 1.36 |
| CCD40 | + | + | − | + | − | 0.61 |
| CCD41 | + | − | − | + | − | 0.92 |
| CCD42 | + | + | + | + | − | 0.64 |
| CCD43 | 0 | 0 | 0 | α | 0 | 0.54 |
| CCD44 | + | − | − | + | + | 1.1 |
| CCD45 | 0 | 0 | 0 | 0 | 0 | 0.79 |
| CCD46 | 0 | 0 | 0 | 0 | −α | 0.54 |
| CCD47 | + | + | + | + | + | 0.94 |
| CCD48 | − | − | + | − | + | 1.32 |
| CCD49 | 0 | 0 | 0 | 0 | 0 | 0.79 |
| CCD50 | − | + | − | − | − | 0.92 |
| CCD51 | α | 0 | 0 | 0 | 0 | 1.51 |
| CCD52 | − | + | + | − | − | 0.92 |

parameters (five in this case). Thus, the value of $\alpha$ for the present study is computed to be 2.378.

The combination of the input parameters and the corresponding SRF values for the CCD analyses has been tabulated in Table 6. Here, the − and + terms represent the factorial points, whereas $\alpha$ corresponds to the axial points. The term 0 represents the mean values corresponding to the center points.

## Formulation of response surface

In order to develop an appropriate response surface, ANOVA has been performed on the SRF values obtained from the CCD analyses. The effect estimates, percentage contribution, and the $p$ value of the linear and quadratic terms for all the factors are evaluated as shown in Table 7. It is observed that linear ($D_1$) and quadratic ($D_1$(Quad)) terms of the dip angle of the first joint set J1 have a significant contribution to the response with the quadratic term showing larger contribution. The next significant contribution is attributed to the friction angle of the joints which characterizes the resistance against instability. The contribution from linear terms $T_1$ of joint set J1 is also comparatively significant. The other terms identified to contribute towards the response are the dip angle $D_2$ and trace length $T_2$ of joint set J2 and the interaction terms $D_1D_2$ which represent the block size and shape formed as a result of intersection of joint sets. In addition, the $p$ value of the above parameters is lower than the significant value (0.05) assumed in the present case confirming the importance of these terms (Montgomery 2013).

**Table 7** ANOVA analysis on the SRF of central composite design (CCD)

| Factor | Effect estimate | Sum of squares | Percentage contribution (%) | $p$ value |
|---|---|---|---|---|
| $D_1$ | − 0.2358 | 0.44 | 14.95 | 0.00 |
| $T_1$ | − 0.1756 | 0.25 | 8.38 | 0.00 |
| $D_2$ | − 0.1138 | 0.1 | 3.48 | 0.00 |
| $T_2$ | − 0.1195 | 0.11 | 3.84 | 0.00 |
| $\phi_j$ | 0.214 | 0.37 | 12.32 | 0.00 |
| $D_1$(Quad) | 0.4025 | 1.3 | 43.57 | 0.00 |
| $T_1$(Quad) | 0.0596 | 0.03 | 0.96 | 0.07 |
| $D_2$(Quad) | 0.0118 | 0.00 | 0.04 | 0.71 |
| $T_2$(Quad) | − 0.0377 | 0.01 | 0.38 | 0.24 |
| $\phi_j$(Quad) | − 0.0624 | 0.03 | 1.05 | 0.06 |
| $D_1T_1$ | − 0.0584 | 0.03 | 0.92 | 0.18 |
| $D_1D_2$ | 0.1159 | 0.11 | 3.61 | 0.01 |
| $D_1T_2$ | − 0.0109 | 0.00 | 0.03 | 0.80 |
| $D_1\phi_j$ | − 0.0828 | 0.05 | 1.84 | 0.06 |
| $T_1D_2$ | 0.0878 | 0.06 | 2.07 | 0.05 |
| $T_1T_2$ | 0.0509 | 0.02 | 0.7 | 0.24 |
| $T_1\phi_j$ | 0.0191 | 0.00 | 0.1 | 0.66 |
| $D_2T_2$ | − 0.0784 | 0.05 | 1.65 | 0.07 |
| $D_2\phi_j$ | − 0.0203 | 0.00 | 0.11 | 0.64 |
| $T_2\phi_j$ | 0.0028 | 0.00 | 0.00 | 0.95 |

Since quadratic term of dip angle along with linear terms associated with the dip, trace length, and joint friction angle has been identified to be significant, hence, a second order equation has been selected to frame the response surface. Equation (11) represents the response surface formulated for the present slope.

$$\begin{aligned} SRF = {} & 1.6 - 0.0798D_1 - 0.315T_1 + 0.0071D_2 + 0.468T_2 + 0.0923\phi_j + 0.000704D_1^2 \\ & + 0.00225T_1^2 - 0.000057D_2^2 - 0.0063T_2^2 + 0.000381\phi_j^2 - 0.000657D_1T_1 + 0.000379D_1D_2 \\ & - 0.000095D_1T_2 - 0.000587D_1\phi_j + 0.001940T_1D_2 + 0.00792T_1T_2 + 0.00013T_1\phi_j - 0.00453D_2T_2 \\ & - 0.00453D_2T_2 - 0.00042D_2\phi_j - 0.00153T_2\phi_j \end{aligned} \quad (11)$$

To verify the effectiveness of the response surface framed on the basis of the CCD analyses, comparison of SRF calculated based on Eq. (11) has been made with the SRF of the numerical models evaluated in the initial factor screening phase (Table 4). The comparison of SRF is presented in Fig. 12 clearly highlighting the effectiveness of the equation in predicting the SRF of the considered slope.

## Variation of SRF with influencing parameters

For better insight into the variation of the behavior of slope characterized by SRF, 3D surface plots have been generated and presented in Fig. 13. The plot shows the variation in SRF as a function of two input parameters

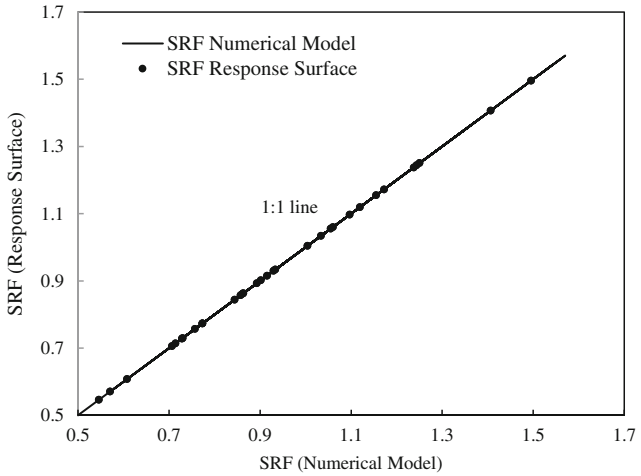


**Fig. 12** Comparison of SRF between numerical analysis and response surface

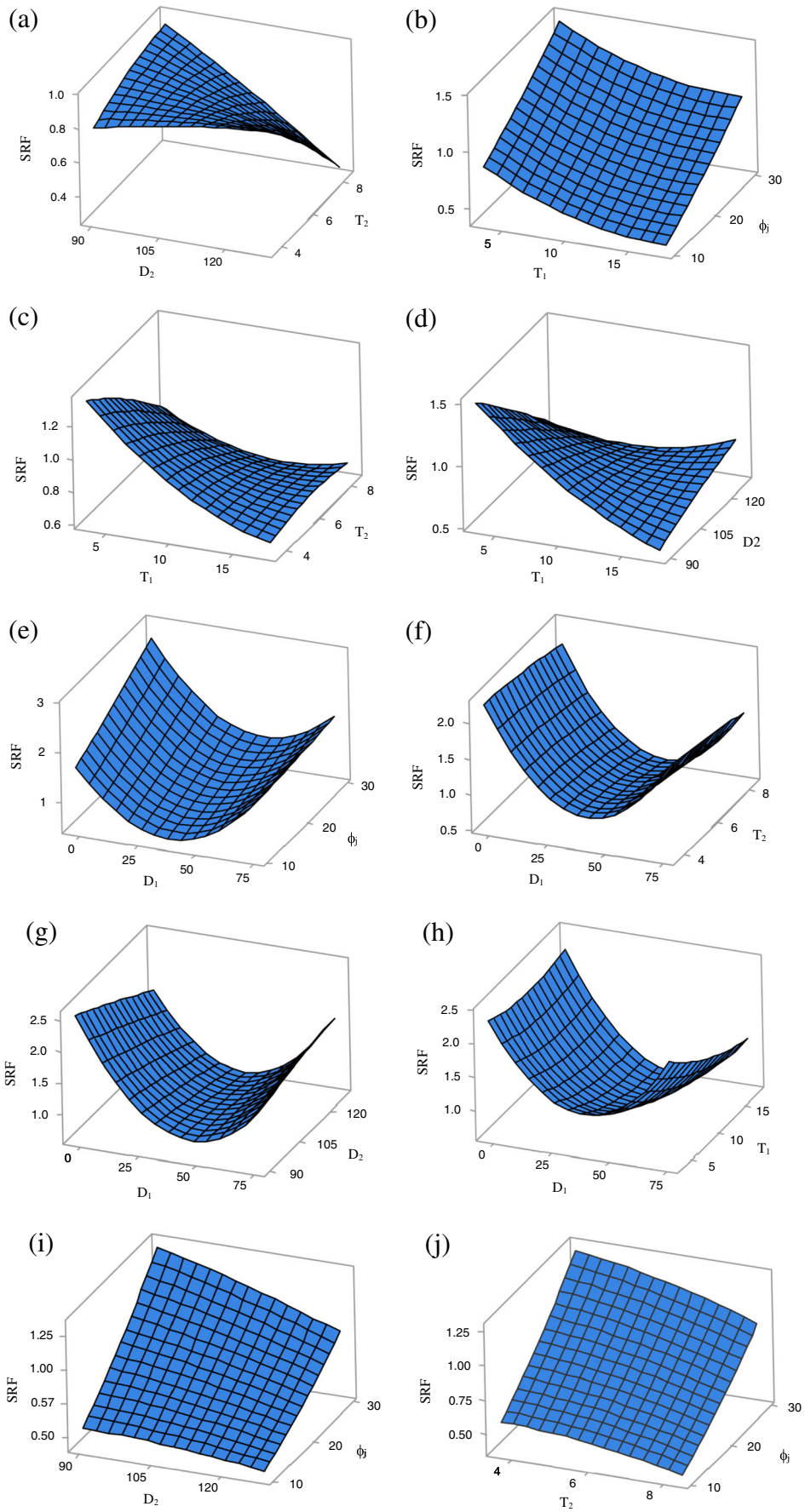


**Fig. 13** **a**–**j** 3D surface plots of random parameters against the SRF of the slope

with all other parameters held constant at their mean values. From Fig. 13e to h, a noticeable curvature may be observed involving parameter $D_1$ suggesting that the SRF decreases with increase in dip angle of up to 50°. With further increase in the dip angle $D_1$, the SRF shows an increase. This is mainly attributed to the interaction of the dip of joint set J1 with the slope angle which is 60°. For dip angle $D_1$ of up to 50°, joint set J1 daylights into the slope, and hence, chances of rock blocks sliding out from the slope are higher.

However, as the dip angle exceeds 50°, joint set J1 becomes almost parallel to the slope lowering the kinematic feasibility of the rock blocks to move out from the slope. This subsequently results in an increase of SRF which is represented by the upward curvature in Fig. 13e to h. The other prominent curvature is observed in Fig. 13a representing the combined effect of dip and trace length of the second joint set. A drop in SRF is observed for higher values of dip angle $D_2$ and trace length $T_2$ highlighting the influence of the second joint set in affecting the slope behavior.

## Application of present methodology in explaining slope behavior

On the basis of the influencing parameters and their combined relative influence identified as discussed in the previous sections, an insight into the slope behavior can be made. The behavior seems to be dominated by the combined action of shearing along both the joint sets as schematically shown in Fig. 14 and their combined interaction. The shearing action causes sliding of rock blocks along joint set J1 coupled with detachment along joint set J2. Depending on the dip angle $D_1$ of joint set J1, there are two possible types of behavior which may be identified from the present study.

Figure 15 provides a schematic representation of the probable behavior when the dip angle $D_1$ is much larger than the friction angle of the joints (i.e., high point estimates). In such cases, sliding along joint set J1 is prominent which dominates the movement of the rock blocks. In such a scenario, the presence of the second joint set J2 facilitates the formation of a release surface which eventually leads to the outward movement. A close view of the discussed behavior is provided in Fig. 16 which shows the response of slope for model run 12 (refer to Table 4). A detailed discussion on this is provided below.

Referring to Table 4, in the case of model run 24, the trace length of joint set J2 has a lower value (lower point estimate) in comparison with model run 16, while the other variables remain identical. As the resistance along the joint sets J1 and J2 is the same in both cases, the difference in SRF result can be explained on the basis that a higher trace length of joint set J2 results in larger block size subsequently leading to higher chances of formation of a release surface. Under the action of the sliding force along joint set J1, detachment of rock block occurs across joint set J2 eventually leading to unstable behavior (refer to Fig. 15). It is thus observed that the SRF in the case of model run 24 is 0.95, whereas for model run 16, it drops to 0.83. Similar reason holds true for the case of model run 24 and model run 28.

To further add to the discussion, the role of the resistive force characterized by the friction angle can be made by comparing model run 16 and model run 32 (refer to Table 4). In both cases, the kinematic feasibility of slope instability remains identical as the geometric parameters of the joint sets and the slope is the same. However, in the case of model run 32, the friction angle of the discontinuity is 16° in comparison with 24° for model run 16. The lower resistance subsequently results in a lower SRF of 0.64 in the case of model run 32 in comparison with model run 16 which has a higher resistance and subsequently a higher SRF of 0.83.

Other prominent behavior observed is associated with the case when the dip of joint set J1 is comparable with the friction angle of the discontinuities. In such cases, detachment and overturning of rock blocks across joint set J2 as shown in Fig. 17 may occur. In fact, a closer view of the results of model run 45 as shown in Fig. 18 confirms this behavior. In this particular case, block detachment and overturning lead to instability and SRF of 0.7. Also a comparison of model run 5 (refer to Table 4) with model run 45 highlights the curvature effect on SRF as highlighted in the response surface plot of $D_2T_2$ as shown in Fig. 13a. The surface plot suggests a sharp decrease in SRF as both $D_2$ and $T_2$ attain respective higher values. Thus, in the case of model run 5, which has a lower trace length, the SRF

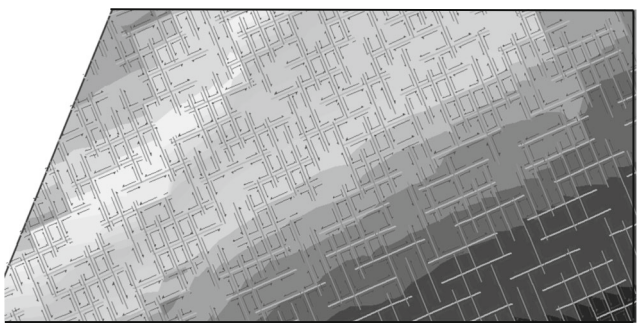

**Fig. 14** Schematic representation of shearing action along both the joint sets

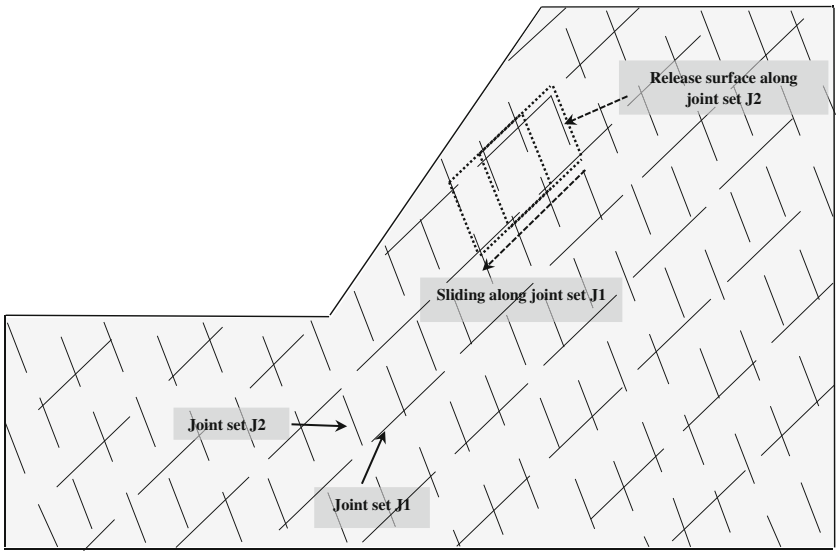


**Fig. 15** Slope response dominated by sliding force along joint set J1

is 1.02 in comparison with SRF of 0.7 in the case of model run 45.

## Summary and discussion

The assessment of stability of jointed rock slope has been a challenging and complex task due to the inherent variability associated with geological medium. Although probabilistic-based approaches have found wide application in slope stability investigations, a rigorous attempt to identify and quantify the relative contribution of various parameters on the integrity of the slope is few in numbers.

In this paper, the influence in variability of both the strength and geometric parameters associated with a jointed rock slope has been investigated. The random parameters considered include the cohesion of the intact rock and the friction angle of both the intact rock and the joint sets. In addition, the variability in geometric parameters characterized by the dip angle and the trace length of the discontinuities has also been taken into account. In order to optimize the process of investigating the combined effects of various parameters on the stability of the slope, concepts of design of experiments (DOE) through factorial design approach have been adopted. A brief description of each component of the adopted methodology implemented in the numerical framework has been provided.

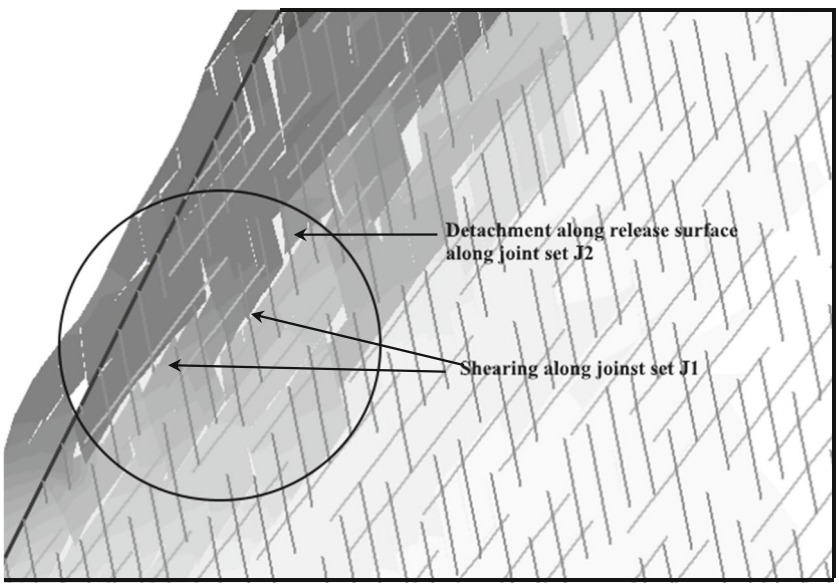


**Fig. 16** Sliding of rock blocks along joint set J1 facilitated by the formation of release surface across joint set J2 (model run 12)

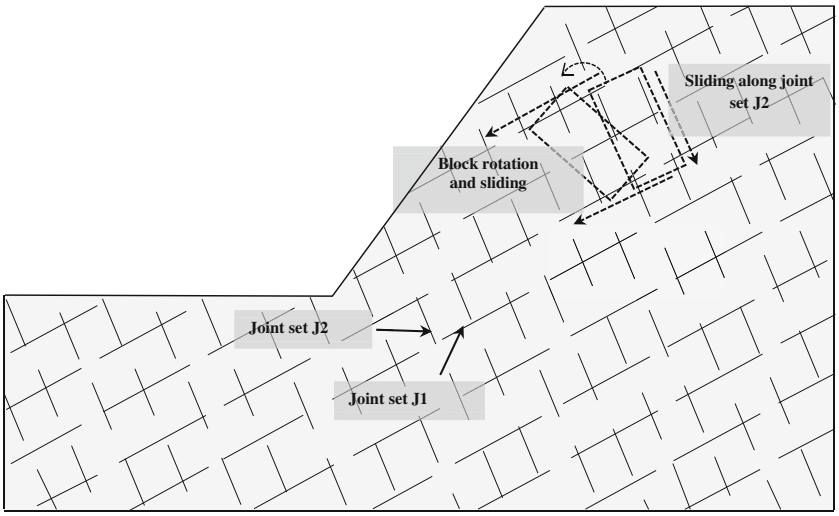


**Fig. 17** Possible mechanism of slope behavior dominated by overturning of rock blocks across joint set J2 in case of shallow dip of joint set J1

Based on the results of the initial factor screening phase, the important factors affecting the behavior of the slope have been identified. It is observed that the performance of a slope with impersistent joints sets is majorly governed by the strength and geometric parameters of the joint sets. Moreover, it is concluded that cohesion and friction angle of intact rock have minimal effect on SRF of the slope configuration considered in the present study. Based on these findings, response surface predicting the SRF of the slope as a function of influencing parameters has been framed using the numerical results from the central composite design (CCD) approach. The response surface framed has shown good agreement with the SRF values evaluated using numerical model runs highlighting its prediction capability. Further, the nature of variation in SRF of the slope with different parameters has also been examined through surface plots.

The present investigation advances the insight into the behavior of the slope by identifying the important parameters and their combined influence. Two dominant types of slope behavior have been identified. When the dip of the first joint set exceeds the joint friction angle, the behavior is mainly governed by the sliding of rock blocks along the first joint set J1 facilitated by the formation of release surface across the second joint set J2. Another dominant behavior observed includes the sliding and overturning of rock blocks along the second joint set. This kind of behavior is observed when the dip of the first joint set becomes comparable with the joint friction angle.

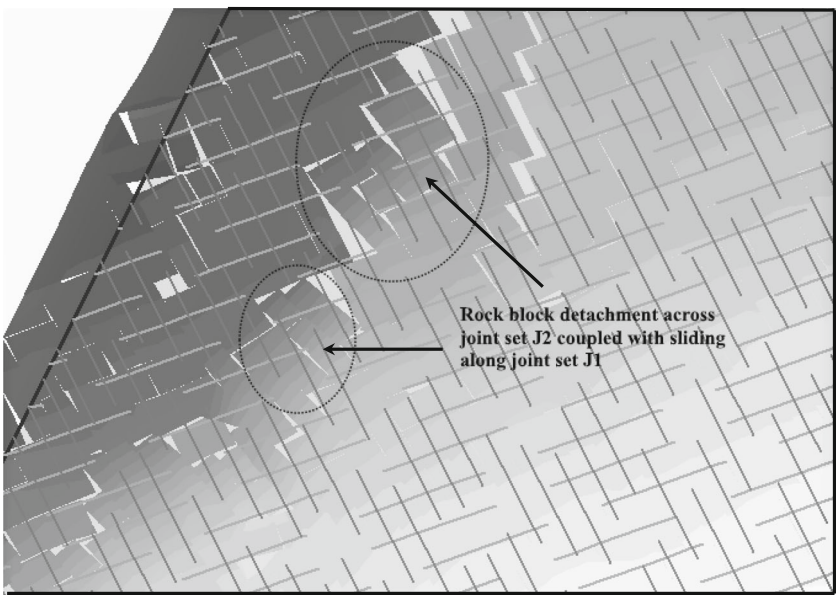


**Fig. 18** Instability driven by the detachment and rotation of rock blocks across joint set J2 (model run 45)

## References


Ahmadabadi M, Poisel R (2016) Probabilistic analysis of rock slopes involving correlated non-normal variables using point estimate methods. Rock Mech Rock Eng 49:909–925

Alemdag S, Akgun A, Kaya A, Gokceoglu C (2014) A large and rapid planar failure: causes, mechanism, and consequences (Mordut, Gumushane, Turkey). Arab J Geosci 7:1205–1221

Baecher GB, Christian JT (2003) Reliability and statistics in geotechnical engineering. Wiley, Chichester

Baecher GB, Lanney NA (1978) Trace length biases in joint surveys. In: Proceedings of the 19th US Symposium on Rock Mechanics, Nevada, 1–3 May 1978

Baecher GB, Lanney NA, Einstein HH (1977) Statistical description of rock properties and sampling. In: Proceeding of the 18th US Symposium on Rock Mechanics, Colorado, 22–24 June 1977

Brideau M, Chauvin S, Andrieux P, Stead D (2012) Influence of 3D statistical discontinuity variability on slope stability conditions. In: Eberhardt et al., editors. In: 11th International and 2nd North American symposium on landslides and engineered slopes, landslides and engineered slopes: protecting society through improved understanding, Banff, Canada

Bridges MC (1976) Presentation of fracture data for rock mechanics. In: Proceedings of the 2nd Australia–New Zealand conference on geomechanics, Brisbane, 21–25 July 1975

Box GEP, Wilson KB (1951) On the experimental attainment of optimum conditions. Roy Statist Soc 13(1):1–45

Cai F, Ugai K (2000) Numerical analysis of the stability of a slope reinforced with piles. Soils Found 40(1):73–84

Cheng YM, Lansivaara T, Wei WB (2007) Two-dimensional slope stability analysis by limit equilibrium and strength reduction methods. Comput Geotech 34(3):137–150

Ching J, Phoon KK, Hu YG (2009) Efficient evaluation of reliability for slopes with circular slip surfaces using importance sampling. J Geotech Geoenviron 135(6):768–777

Christian JT, Ladd CC, Baecher GB (1994) Reliability applied to slope stability analysis. J Geotech Eng 120(12):2180–2207

Crozier MJ (1986) Landslides: causes, consequences and environment. Croom Helm Pub, London, p 252

Dawson EM, Roth WH, Drescher A (1999) Slope stability analysis by strength reduction. Geotechnique 49(6):835–840

Dershowitz WS, Einstein HH (1988) Characterizing rock joint geometry with joint system models. Rock Mech Rock Eng 21:21–51

Donald IB, Giam SK (1988) Application of the nodal displacement method to slope stability analysis. In: Proceedings of the 5th Australia–New Zealand conference on geomechanics, Sydney, Australia, 456: 460

Duncan JM (2000) Factors of safety and reliability in geotechnical engineering. J Geotech Geoenviron 126(4):307–316

Duzgun HSB, Bhasin RK (2009) Probabilistic stability evaluation of Oppstadhornet Rock Slope Norway. Rock Mech Rock Eng 42(5): 729–749

Duzgun HSB, Yucemen MS, Karpuz C (2003) A methodology for reliability-based design of rock slopes. Rock Mech Rock Eng 36(2):95–120

Ehlen J (2002) Some effects of weathering on joints in granitic rocks. Catena 49:91–109

Fahimifar A, Abdolmaleki A, Soltani P (2012) Stabilization of rock slopes using geogrid boxes. Arab J Geosci 7:609–621

Fookes PG, Wilson DD (1966) The geometry of discontinuities and slope failures in Siwalik Clay. Geotechnique 16(4):305–320

Grelle G, Revellino P, Donnarumma A, Guadagno FM (2011) Bedding control on landslides: a methodological approach for computer-aided mapping analysis. Nat Hazards Earth Syst Sci 11:1395–1409

Griffiths DV, Lane PA (1999) Slope stability analysis by finite elements. Geotechnique 49(3):387–403

Griffiths DV, Lin H, Cao P (2010) A comparison of numerical algorithms in the analysis of pile reinforced slopes. Proc Geo Florida 2010 Conf, West Palm Beach, Florida 1:175–183

Gumede H, Stacey TR (2007) Measurement of typical joint characteristics in South African gold mines and the use of these characteristics in the prediction of rock falls. JS Afr I Min Metall 107:335–344

Gunther A (2003) SLOPEMAP: programs for automated mapping of geometrical and kinematical properties of hard rock hill slopes. Comput Geosci 29:865–875

Guzzetti F, Cardinali M, Reichenbach P (1996) The influence of structural setting and lithology on landslide type and pattern. Environ Eng Geosci 2(4):531–555

Hammah RE, Yacoub TE, Curran JH. (2009). Numerical modelling of slope uncertainty due to rock mass jointing. In: International conference on rock joints and jointed rock masses, Tucson, USA

Hong HP (1996) Point-estimate moment-based reliability analysis. Civ Eng Environ Syst 13(4):281–294

Hong HP (1998) An efficient point estimate method for probabilistic analysis. Reliab Eng Syst Saf 59(3):261–267

Hudson JA, Priest SD (1983) Discontinuity frequency in rock masses. Int J Rock Mech Min Sci 20(2):73–89

Juang CH, Jhi YY, Lee DH (1998) Stability analysis of existing slopes considering uncertainty. Eng Geol 49(2):111–122

Koukis G, Ziourkas C (1991) Slope instability phenomena in Greece: a statistical analysis. Bull Int Assoc Eng Geol 43:47–60

Lee YF, Chi YY, Juang CH, Lee DH (2012) Reliability analysis of rock wedge stability - a knowledge-based clustered partitioning (KCP) approach. J Geotech Geoenviron 138(6):700–708

Li DQ, Chen YF, Lu WB, Zhou CB (2011) Stochastic response surface method for reliability analysis of rock slopes involving correlated non-normal variables. Comput Geotech 38(1):58–68

Low BK (1997) Reliability analysis of rock wedges. J Geotech Geoenviron 123(6):498–505

Low BK (2007) Reliability analysis of rock slopes involving correlated non normals. Int J Rock Mech Min Sci 44(6):922–935

Low BK (2008) Efficient probabilistic algorithm illustrated for a rock slope. Rock Mech Rock Eng 41(5):715–734

Low BK, Einstein HH (1992) Simplified reliability analysis for wedge mechanisms in rock slopes. Proc., 6th Int. Symp. on Landslides. Balkema, Rotterdam, the Netherlands, pp. 499–507

Matsui T, San K-C (1992) Finite element slope stability analysis by shear strength reduction technique. Soils Found 32(1):59–70

Meyer T, Einstein HH (2002) Geologic stochastic modeling and connectivity assessment of fracture systems in the Boston area. Rock Mech Rock Eng 35(1):23–44

Montgomery D (2013) Design and analysis of experiments. John Wiley and Sons, New York

Mostyn GR, Li KS (1993) Probabilistic slope analysis—state of play. Proceedings of Conference on Probabilistic Methods in Geotechnical Engineering. A.A Balkema, Canberra, Australia, pp. 89–109

Myers RH, Montgomery DC, Anderson-Cook CM (2009) Response surface methodology: process and product optimization using designed experiments. 3rd edition. Wiley, New York

Myers RH, Montgomery DC, Vining GG, Borror CM, Kowalski SM (2004) Response surface methodology: a retrospective and literature survey. J Qual Technol 36:53–77

Nilsen B (2000) New trend in rock slope stability analysis. Bull Eng Geol Environ 58:173–178

Oka Y, Wu TH (1990) System reliability on slope stability. J Geotech Eng 116(8):1185–1189

Park HJ, West TR (2001) Development of a probabilistic approach for rock wedge failure. Eng Geol 59(3–4):233–251

Park HJ, West TR, Woo I (2005) Probabilistic analysis of rock slope stability and random properties of discontinuity parameters, Interstate Highway 40. Eng Geol 79(3–4):230–250

Park HJ, Um JG, Woo I, Kim JW (2012) Application of fuzzy set theory to evaluate the probability of failure in rock slopes. Eng Geol 125: 92–101

Pathak S, Nilsen B (2004) Probabilistic rock slope stability analysis for Himalayan condition. Bull Eng Geol Environ 63:25–32

Priest SD (1993) Discontinuity analysis for rock engineering. Chapman and Hall, New York

Priest SD, Hudson JA (1976) Discontinuity spacing in rock. Int J Rock Mech Min Sci 13:135–148

Rathod GW, Rao KS (2012) Finite element and reliability analyses for slope stability of Subansiri Lower Hydroelectric Project: a case study. Geotech Geol Eng 30:233–252

Rocscience Inc., RS 2.0 (2015) Finite element analysis for excavations and slopes, Toronto, Canada

Rosenblueth E (1975) Point estimates for probability moments. Proc Natl Acad Sci USA 72:3812–3814

Shamekhi E, Tannant DD (2015) Probabilistic assessment of rock slope stability using response surfaces determined from finite element models of geometric realizations. Comput Geotech 69:70–81

Shooshpasha I, Amirdehi HA (2015) Evaluating the stability of slope reinforced with one row of free head piles. Arab J Geosci 8:2131–2141

Song KI, Cho GC, Lee SW (2011) Effects of spatially variable weathered rock properties on tunnel behaviour. Prob Eng Mech 26:413–426

Maerz NH, Youssef AM, Pradhan B, Bulkhi A (2015) Remediation and mitigation strategies for rock fall hazards along the highways of Fayfa Mountain, Jazan Region, Kingdom of Saudi Arabia. Arab J Geosci 8:2633–2651

Naylor D (1982) Finite elements and slope stability. Numerical methods in geomechanics: proceedings of the NATO Advanced Study Institute, University of Minho, Braga, Portugal, held at Vimeiro, August 24–Sept. 4, 1981, 229: 244

Ugai K, Leshchinsky D (1995) Three-dimensional limit equilibrium and finite element analysis: a comparison of result. Soils Found 35(4):1–7

Vanmarcke EH (1980) Probabilistic stability analysis of earth slopes. Eng Geol 16(1–2):29–50

Varnes DJ (1978) Slope movement, types and processes. In: Landslides analysis and control, Schuster RL, Krizek RJ (Eds) Transportation Research Board. National Academy of Sciences, Washington, pp 11–33, Special Report 176

Warburton PM (1980) Stereological interpretation of joint trace data: influence of joint shape and implications for geological surveys. Int J Rock Mech Min Sci 17(6):305–316

Wei WB, Cheng YM (2009) Strength reduction analysis for slope reinforced with one row of piles. Comput Geotech 36(7):1176–1185

Wei WB, Cheng YM, Li L (2009) Three-dimensional slope failure analysis by the strength reduction and limit equilibrium methods. Comput Geotech 36:70–80

Weiss M (2008) Techniques for estimating fracture size: a comparison of methods. Int J Rock Mech Min Sci 45:460–466

Won J, You K, Jeong S, Kim S (2005) Coupled effects in stability analysis of pile–slope systems. Comput Geotech 32(4):304–315

Wyllie DC, Mah CW (2004) Rock slope engineering, 4th Edition. Spon Press, Taylor and Francis Group

Yang S, Ren X, Zhang J (2011) Study on embedded length of piles for slope reinforced with one row of piles. J Rock Mech Geotech Eng 3(2):167–178

Youssef AM, Pradhan B, Al-Harthi SG (2015) Assessment of rock slope stability and structurally controlled failures along Samma escarpment road, Asir region (Saudi Arabia). Arab J Geosci 8:6835–6852

Youssef AM, Pradhan B, Maerz NH (2014) Debris flow impact assessment caused by 14 April 2012 rainfall along the Al-Hada Highway, Kingdom of Saudi Arabia using high-resolution satellite imagery. Arab J Geosci 7:2591–2601

Zadhesh J, Jalali SME, Ramezanzadeh A (2014) Estimation of joint trace length probability distribution function in igneous, sedimentary, and metamorphic rocks. Arab J Geosci 7:2353–2361

Zhang K, Cao P, Meng J, Li K, Fan W (2015) Modeling the progressive failure of jointed rock slope using fracture mechanics and strength reduction method. Rock Mech Rock Eng 48:771–785

Zienkiewicz OC, Humpheson C, Lewis RW (1975) Associated and non-associated visco-plasticity and plasticity in soil mechanics. Geotechnique 25(4):671–689